Title
GRAPHICAL CALCULATION OF WAIST-TO-WAIST TRANSFER IN PARTICLE OPTICS

Author
Luccio, A.U.

Publication Date
1969-09-01

Submitted to Nuclear Instruments and Methods

UCRL-18977
Preprint

GRAPHICAL CALCULATION OF WAIST-TO-WAIST TRANSFER IN PARTICLE OPTICS

A. U. Luccio

September 1969

AEC Contract No. W-7405-eng-48

LAWRENCE RADIATION LABORATORY
UNIVERSITY of CALIFORNIA BERKELEY

UCRL-18977

DISCLAIMER

GRAPHICAL CALCULATION OF WAIST-TO-WAIST TRANSFER IN PARTICLE OPTICS[†]

A. U. Luccio[‡]

Lawrence Radiation Laboratory
University of California
Berkeley, California 94720

September 1969

Abstract

A graphical method is described to calculate waist-to-waist transfer in thin-lens particle optics. Examples are given to show how the method would allow one to design a beam line with great speed and reasonable precision.

[†]This work was performed under the auspices of the U. S. Atomic Energy Commission.

[‡]On leave of absence from the University of Milan, Milan, Italy.

Perhaps the most important result of an optical transfer line calculation for charged particles is the location of the "waists" or minima in the beam section and the determination of their phase-space shape. Formulas for waist-to-waist transfer in thin-lens optics are given e.g. in A. P. Banford's book[1]). These formulas are quite general, since all optical elements, such as lenses, beam bending devices, etc. can be reduced to appropriate systems of thin lenses and drift spaces[2]). Unfortunately, if the elements are many, the use of these formulas is rather tedious, because of the large number of parameters to be adjusted and very often becomes impossible in practice.

The procedure can be greatly expedited by the use of charts and nomograms, of which good examples are due to Banford[3]), Smith[4]), Randle[5], and Resmini[6]). If the line contains some accelerating element, however, the above methods cannot be utilized and it appeared desirable to us to develop a very general method for waist-to-waist transfer calculation. In doing so, our aim has been that of simplicity of reading and use, so that the fundamental properties of waists could appear as explicitly as possible. The results of graph calculations are accurate enough for many purposes and, in any case, can be considered as a good starting point for more refined computer calculations.

The graphs presented here are an improved and generalized version of a method already described[7]).

Waist-to-Waist Transfer for a Thin Accelerating Lens

Let us refer the beam in a meridian section to the axis Z, longitudinal and y transverse (fig. 1). Subscripts 1 and 2 will mean upstream and downstream from a lens, subscript 0 will be referred to a waist.

The following definitions will be used:

y_0, y_0'	phase-space coordinate of a waist
$\varepsilon = y_0 y_0'$	emittance of a waist
$X = y_0/y_0'$	characteristic length of a waist
$\mu = y_{02}/y_{01}$	linear magnification
z_1, z_2	distances of a point from the lens, upstream and downstream
z_{01}, z_{02}	distances of the waists from the lens ($z_0 < 0$ will correspond to a virtual waist)
f	focal length (positive for a converging lens)
$\eta^2 = V_2/V_1$	acceleration factor .

The thin lens we are discussing will be considered as composed of a thin nonaccelerating lens (L) followed or preceded by a thin accelerating gap (A), which changes the energy eV_1 of an incoming particle into eV_2. This lens changes the emittance of the beam, and therefore the characteristic length of the second waist, in the following way:

$$\varepsilon_2 = \varepsilon_1/\eta$$
$$X_2 = \mu^2 \eta X_1 \quad . \tag{1}$$

In matrix notations, a field-free (drift = D) space can be represented by

$$D = \begin{pmatrix} 1 & z \\ 0 & 1 \end{pmatrix} ,$$

while a thin nonaccelerating lens is represented by

$$L = \begin{pmatrix} 1 & 0 \\ -1/f & 1 \end{pmatrix} .$$

Across the accelerating gap, the x component of the phase-space representation of the beam is not changed, while for the x' component it is

$$x'_2 = \frac{P_x}{P_2} = \frac{P_x}{P_1}\frac{P_1}{P_2} = \frac{x'_1}{\eta}$$

$$P^2 = 2mqV$$

Accordingly, the matrix for the accelerating gap can be written

$$A = \begin{pmatrix} 1 & 0 \\ 0 & 1/\eta \end{pmatrix} \quad .$$

For a lens <u>followed</u> by A, the overall transfer matrix is

$$M = DALD = \begin{pmatrix} 1 & z_2 \\ 0 & 1 \end{pmatrix} \begin{pmatrix} 1 & 0 \\ 0 & 1/\eta \end{pmatrix} \begin{pmatrix} 1 & 0 \\ -1/f & 1 \end{pmatrix} \begin{pmatrix} 1 & z_1 \\ 0 & 1 \end{pmatrix}$$

$$= \begin{pmatrix} 1 - z_2/\eta f & z_1 + z_2/\eta - (z_1 z_2)/\eta f \\ -1/\eta f & 1/\eta - z_1/\eta f \end{pmatrix} \quad .$$

The equations

$$\begin{cases} \begin{pmatrix} 0 \\ y'_2 \end{pmatrix} = DALD \begin{pmatrix} y_1 \\ 0 \end{pmatrix} \\ \begin{pmatrix} y_2 \\ 0 \end{pmatrix} = DALD \begin{pmatrix} 0 \\ y'_1 \end{pmatrix} \end{cases}$$

can be used to find the relationship between f and the measurable focal lengths before and after the lens. The result* is

---

*Analogously, for a thin nonaccelerating lens preceded by A, one obtains

$$\begin{cases} f_1 = f/\eta \\ f_2 = f \quad . \end{cases} \qquad (M = DLAD) \qquad (3')$$

$$\begin{cases} f_1 = f \\ f_2 = \eta f \end{cases} . \qquad (M = DALD) \qquad (3)$$

The transport equations, waist-to-waist, can be written explicitly, with y_{01} and y_{02} in the place of y_1 and y_2:

$$\begin{cases} y_2 = M_{11}(z_{02})y_1 + M_{12}(z_{01},z_{02})\, y_1' \\ y_2' = M_{21}y_1 + M_{22}(z_{01})y_1' \end{cases} .$$

At a waist, we can choose y, y' as coordinates of points on the contour of upright phase-space ellipses; namely:

$$\frac{y^2}{y_0^2} + \frac{y'^2}{y_0'^2} = 1, \qquad \text{or } y^2 + X^2 y'^2 + y_0^2 \qquad (5)$$

Squaring and summing the two equations (4) with the conditions (5), and equating the coefficients of y_1^2, $y_1'^2$, and $y_1 y_1'$, one obtains

$$\begin{cases} \left(1 - \frac{z_{02}}{\eta f}\right)^2 + \frac{X_2^2}{\eta^2 f^2} = \mu^2 \\ \left(z_{01} + \frac{z_{02}}{\eta} - \frac{z_{01}z_{02}}{\eta f}\right)^2 + \left(\frac{1}{\eta} - \frac{z_{01}}{\eta f}\right)^2 X_2^2 = \mu^2 X_1^2 \\ \left(1 - \frac{z_{02}}{\eta f}\right)\left(z_{01} + \frac{z_{02}}{\eta} - \frac{z_{01}z_{02}}{\eta f}\right) - \left(\frac{1}{\eta} - \frac{z_{01}}{\eta f}\right)\frac{X_2^2}{\gamma f} = 0 \end{cases}$$

which are satisfied by

$$\mu^2 = \frac{z_{02} - \eta f}{\eta(z_{01} - f)}$$

$$f^2 = \mu^2[(x_{01} - f)^2 + X_1^2] \qquad (6)$$

Equations (6) reduce to Banford's equations for $\eta = 1$ (no acceleration).

It is convenient to rearrange eq. (6) in the following fashion:

$$\begin{cases} z_{02} = \eta f \dfrac{(z_{01}-f)z_{01} + X_1^2}{(z_{01}-f)^2 + X_1^2} \\ \mu^2 = \dfrac{f^2}{(z_{01}-f)^2 + X_1^2} \end{cases} \qquad (6')$$

Equations (6') together with eq. (1) can be used to design a transport line, from the starting values of

$$\varepsilon_1, X_1 \text{ or } \mathcal{Y}_{01}, \mathcal{Y}'_{01} \quad ,$$

which determine completely the initial phase-space configuration of the beam.

The Effect of Finite Emittance

Often point-source Gaussian optics considerations are useful in calculating a beam line. This, however, can lead to wrong results, if the transition between point and finite emittance optics is not made clear.

To show explicitly the role played by the emittance, let us rewrite the (6') in the following dimensionless form:

$$\begin{cases} t = \dfrac{s(s-1) + \alpha^2}{(s-1)^2 + \alpha^2} \\ \mu^2 = \dfrac{1}{(s-1)^2 + \alpha^2} \end{cases} \quad , \qquad (6'')$$

with the definitions:

$$s = \frac{z_{01}}{f} \; , \quad t = \frac{z_{01}}{\eta f} \; , \quad \alpha = \frac{X_1}{f} \quad .$$

The behavior of the functions $t(s,\alpha)$ and $|\mu|^2(s,\alpha)$ is sketched in figs. 2 and 3.

The formulas derived so far must reduce to the classical ones for thin-lens--point-object optics. In the classical limit,

$\alpha << 1, s, s-1,$

we have, to second order in α/s and $\alpha/(s-1)$,

$$\begin{cases} \frac{1}{s} + \frac{1}{t} = 1 + \frac{\alpha^2}{s^2(s-1)} \\ \mu = \frac{1}{s-1}\left(1 - \frac{\alpha^2}{2(s-1)^2}\right) \end{cases} . \tag{7}$$

For $\eta = 1$, eqs. (7) become

$$\frac{1}{z_{01}} + \frac{1}{z_{02}} = \frac{1}{f}\left(1 + \frac{f}{z_{01}-f}\frac{X_1^2}{z_{01}^2}\right) = \frac{1}{f}\left(1 + \frac{z_{02}}{z_{01}}\frac{X_1^2}{z_{01}^2}\right)$$

$$\mu = \frac{f}{z_{01}-f}\left(1 - \frac{X_1^2}{2(z_{01}-f)^2}\right) = \frac{z_{02}}{z_{01}}\left(1 - \frac{1}{2}\left(\frac{z_{01}+z_{02}}{z_{01}}\right)^2\frac{X_1^2}{z_{01}^2}\right) . \tag{8}$$

In (8) the finite emittance corrections appear explicitly through X_1.

Graphical Solution of the W-W Transfer Equations

It is convenient to rearrange eqs. (1) and (6') by making use of the new set of definitions:

$$u = \frac{z_{01}}{X_1} , \quad v = \frac{z_{02}}{X_1} , \quad \text{and } \phi = \frac{f}{X_1} ,$$

in the following form

$$\begin{cases} X_2 = \mu^2 \eta X_1 \\ v = \eta\phi \dfrac{u(u-\phi) + 1}{(u-\phi)^2 + 1} \\ \mu^2 = \dfrac{\phi^2}{(u-\phi)^2 + 1} \end{cases} \qquad (9)$$

The function $\frac{v(u,\phi)}{\eta}$ is plotted in figs. 4 and 5 (for positive values of u, real upstream waists) and in fig. 6 (negative u values, virtual upstream waists). It is easy to recognize that such negative values exist only for $\phi > 2$.

The function $\mu^2(u,\phi)$ is plotted in figs. 7 and 8.

The graphs can be used quite generally to deal with real and virtual waists and with converging and diverging lenses. In this last case ($\phi < 0$) from (9) it follows:

$$\begin{cases} v(u,-\phi) = -v(-v,\phi) \\ \mu^2(u,-\phi) = {}^2(-u,\phi) \end{cases} \quad . \qquad (10)$$

The following well known features of W-W transfer show clearly from the graphs:

Figs. 4 and 5: to a given position of the source waist, there corresponds a focal length for which v, positive or negative, is maximum. Locus of maxima is indicated by the dashed lines. This is an important property; it means e.g. that in order to obtain a real image waist at a given position downstream, the source waist should be located not too close to the lens, upstream.

Fig. 6: to a virtual source waist ($u < 0$) it never corresponds a virtual image waist, ($v < 0$). This is obvious, but it is useful to remember while using the graphs for an actual calculation.

Fig. 7: the magnification μ^2 has a maximum for each positive u, corresponding to a definite focal length. Locus of maxima shown by a dashed line.

Fig. 8: again a quite obvious property: if $u < 0$ and ϕ is positive, μ^2 is less than 1.

Examples

Let us show on two examples the use of the graphs.

In fig. 9 is sketched a line composed by an ion gun with proper (accelerating) optics, plus another (nonaccelerating) lens, e.g., an "Einzel" lens. The purpose of the line is to transfer a crossover (waist) of given characteristics near the ion source to a given point at a given distance. If we refer to the geometrical data of fig. 9 and to the following properties of the starting waist:

$$y_{01} = 0.5 \text{ cm} \qquad \varepsilon_1 = 0.05 \text{ cm-rad}$$

$$y'_{01} = 0.100 \text{ rad} \qquad X_1 = 5 \text{ cm} \quad ,$$

the calculation can run as follows:

First lens. For $\eta = 2$, $z_{01} = 10$ cm and accordingly for

$$u = \frac{z_{01}}{X_1} = 10:5 = 2$$

a reasonable value for z_{02}, corresponding to a second waist midway between the first and the second lens, is: $z_{02} = 24$ cm. This value corresponds to

$$\frac{v}{\eta} = \frac{z_{02}}{\eta X_1} = 2.4$$

which can be obtained from the graph of fig. 6 with

$\phi = 1.5$; or $f = 7.5$ cm, $f_2 = 15$ cm.

The corresponding values for μ^2 and X_2 obtained from the graph of fig. 7 are

$\mu^2 = 1.8$, $X_2 = \mu^2 \eta X_1 = 18$ cm.

Second lens. For $\eta = 1$, $z_{01} = 25$ cm and accordingly for

$$u = \frac{z_{01}}{X_1} = 25:18 = 1.4 \quad ,$$

we can obtain (fig. 6) a value $z_{02} = 21$ cm, or $\frac{v}{\eta} = \frac{z_{02}}{\eta X_1} = 21:18 = 1.17$,

with $\phi = 0.95$; or $f = f_2 = 17$ cm;
the resulting magnification (fig. 7) is $\mu^2 = 0.8$;
the overall magnification is $\mu_{ov} = (0.8\times 1.8)^{1/2} = 1.2$;
and the final emittance is $\varepsilon_{ov} = \varepsilon_{in}/\eta = 0.025$ cm-rad.

As a second example let us consider a beam bending line arrangement composed by a 15°9 bending magnet with 15°3 focusing edges followed by a quadrupole pair (fig. 10). The purpose of the system is to produce a waist both radially and axially at a given distance downstream after the doublet. For the sake of comparison the optics for this case has been calculated with the computer program TRAN 2 (ref. 8). The procedure to calculate the line and the agreement with the computer results are shown in table 1.

References

1. A. P. Banford, "The transport of charged particle beams," (E. and F. N. Spon, Ltd., London, 1966).

2. Ibid. p. 40.

3. A. P. Banford "A circle diagram for beam transport calculations," Report NIRL/R/8 (Rutherford Laboratory, 1961).

4. W. I. B. Smith "Beam transport calculations using graphs" Report CEAL-1002 (MIT 1963).

5. T. C. Randle "Two graphical constructions for beam transport problems," Nucl. Instr. Methods 41 (1966) 319.

6. F. G. Resmini, "A simple method for determining waist-to-waist transfer properties of quadrupole doublets and triplets," Nucl. Instr. Methods 68 (1969) 235.

7. A. U. Luccio "Waist-to-waist transfer in thin lens optics," Lawrence Radiation Laboratory Report UCRL-18217 (May 1968).

8. A. C. Paul, "UCLRL TRANSPORT" Program TRAN 2, (LRL-January 5-1969).

TABLE 1

Calculation of a system composed by an α = 14°9 bending magnet with β = 15°3 focusing edges, followed by a quadrupole doublet. Curvature radius in the B.M. r = 150 cm, focal lengths as shown. s = separation between elements as shown. Units: s, z, f, y in cm, y' in rad. The values in parentheses are results of computer calculations[8]). Compare with fig. 10.

	s	$z_{01}=s-z_{02}$	f	$u = z_{01}/X$	$\phi = f/X$	v (fig.)	μ^2 (fig.)	$z_{02} = vX$	$X := \mu^2 X$	$y := \mu y$	$y' := y/X$
		Axial ("vertical") beam						0.	25.	0.25	0.010
15°3 Edge	70	70.	+549.	2.8	22	-3.2 (5)	1.3 (7)	-80.	32.5	0.285	0.0088 (0.008737)
15°3 Edge	39.2	119.2	+549	3.67	16.9	-4.4 (5)	2. (7)	-143.	65.	0.403	0.0062 (0.006884)
Q_I	115.	258.	-49.	3.97	-0.753	-0.61(6)	0.025(8)	-39.6	1.60	0.064	0.040 (0.043883)
Q_{II}	60.	99.6	+58 (+60)	62.	36.	87. (4)	1.8 (7)	141. (145.)	2.88	0.085 (0.082)	0.0295 (0.030405)
		Total axial length = 425.2 (429.20)									
		Radial ("horizontal") beam						0.	25.	0.25	0.010
15°3 Edge	70.	70.	-549.	2.8	-22.	-2.4 (6)	0.78 (8)	-60.	19.5	0.221	0.0113 (0.011284)
14°9 B.M.	19.6	79.6	+580	4.08	29.7	-5.3 (5)	1.3 (7)	-103.3	25.4	0.252	0.0099 (0.009691)
15°3 Edge	19.6	122.9	-549.	4.83	-21.6	-3.9 (6)	0.7 (8)	-99.	17.8	0.211	0.0118 (0.11728)
Q_I	115.	214.	+65.9	12.	3.7	5.2 (4)	0.2 (7)	92.5	3.56	0.094	0.265 (0.26350)
Q_{II}	60.	-32.5	-40. (-43.4)	-9.13	-11.2	38. (5)	25. (7)	137. (145.)	89.	0.473 (0.442)	0.0053 (0.005658)
		Total radial length = 421.2 (429.20)									

Figure Captions

Fig. 1. A thin accelerating lens.

Fig. 2. The function $t(s,\alpha)$ and its point-optics limit.

Fig. 3. The function $|\mu|(s,\alpha)$ and its point-optics limit.

Fig. 4. The function $v(u,\phi) > 0$ for $u > 0$.

Fig. 5. The function $v(u,\phi) < 0$ for $u > 0$.

Fig. 6. The function $v(u,\phi) > 0$ for $u < 0$.

Fig. 7. The magnification function $\mu^2(u,\phi)$ for $u > 0$.

Fig. 8. The magnification function $\mu^2(u,\phi)$ for $u < 0$.

Fig. 9. Example I of application.

Fig. 10. Example II of application. Solid line: graph calculation, dashed line: computer solution. Drawing not on scale.

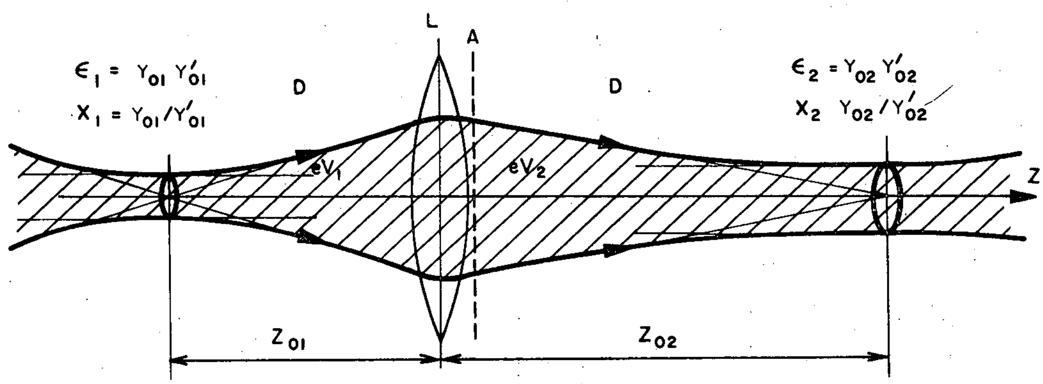

XBL684-2601

Fig. 1

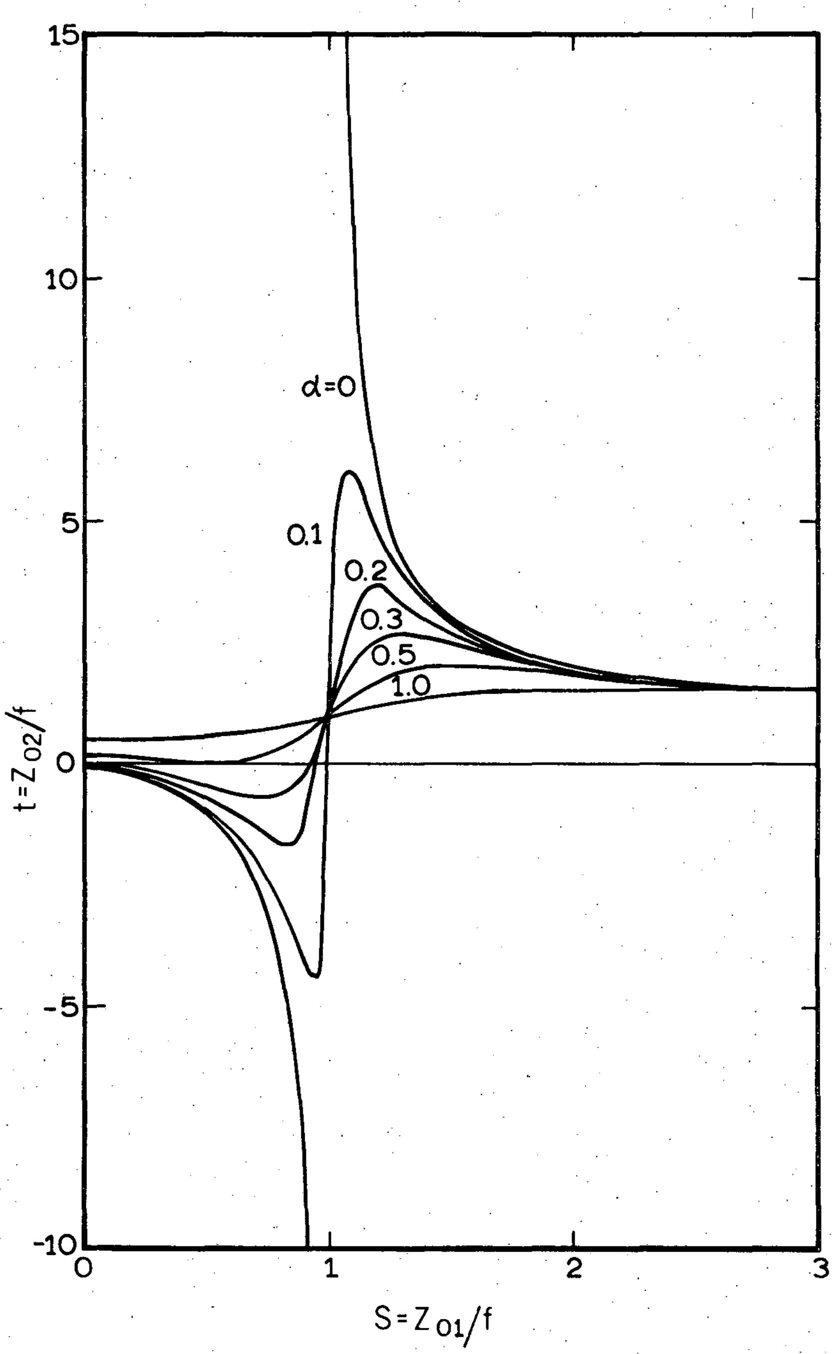

XBL 692 4801

Fig. 2

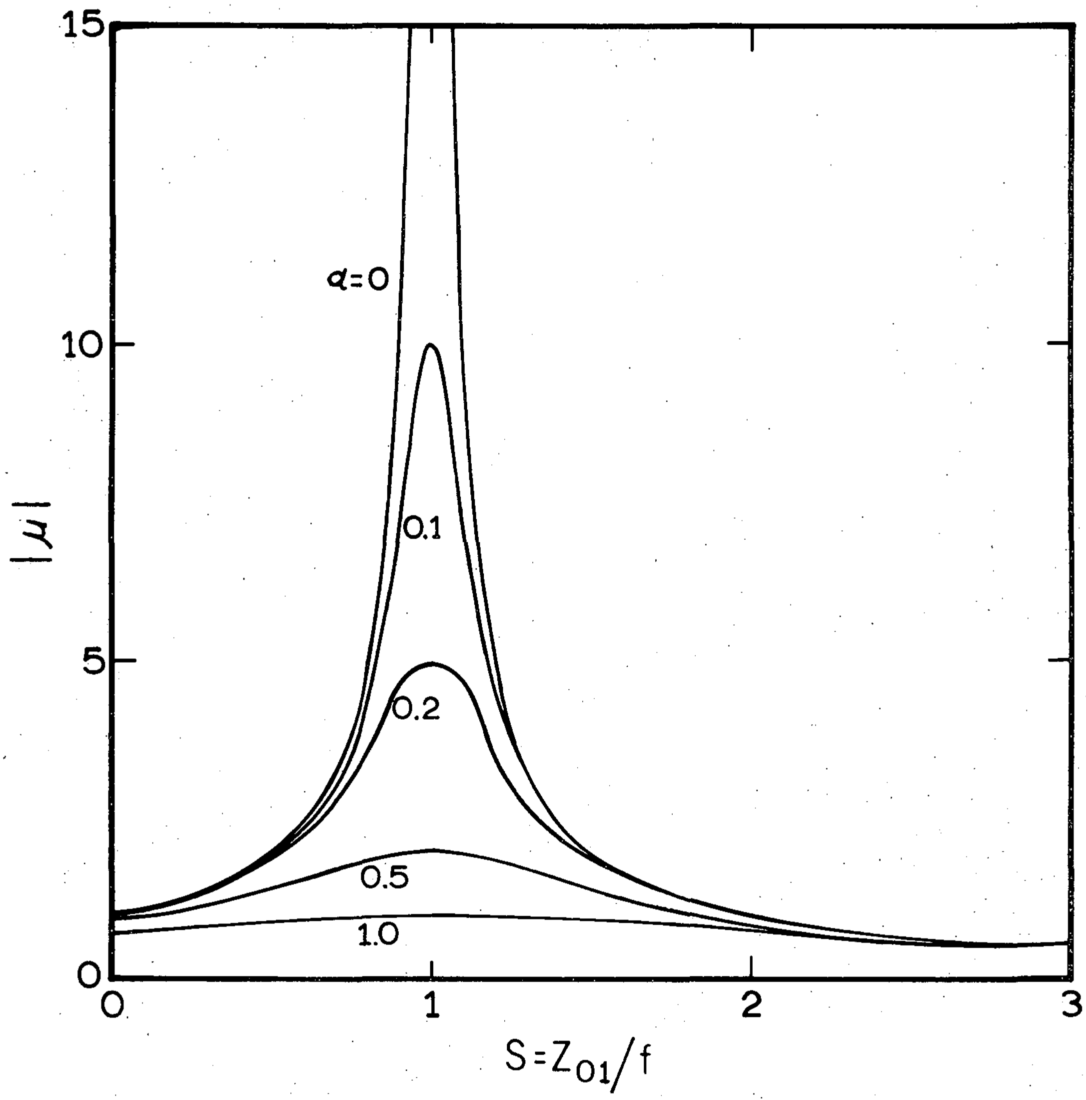

XBL 692 4500

Fig. 3

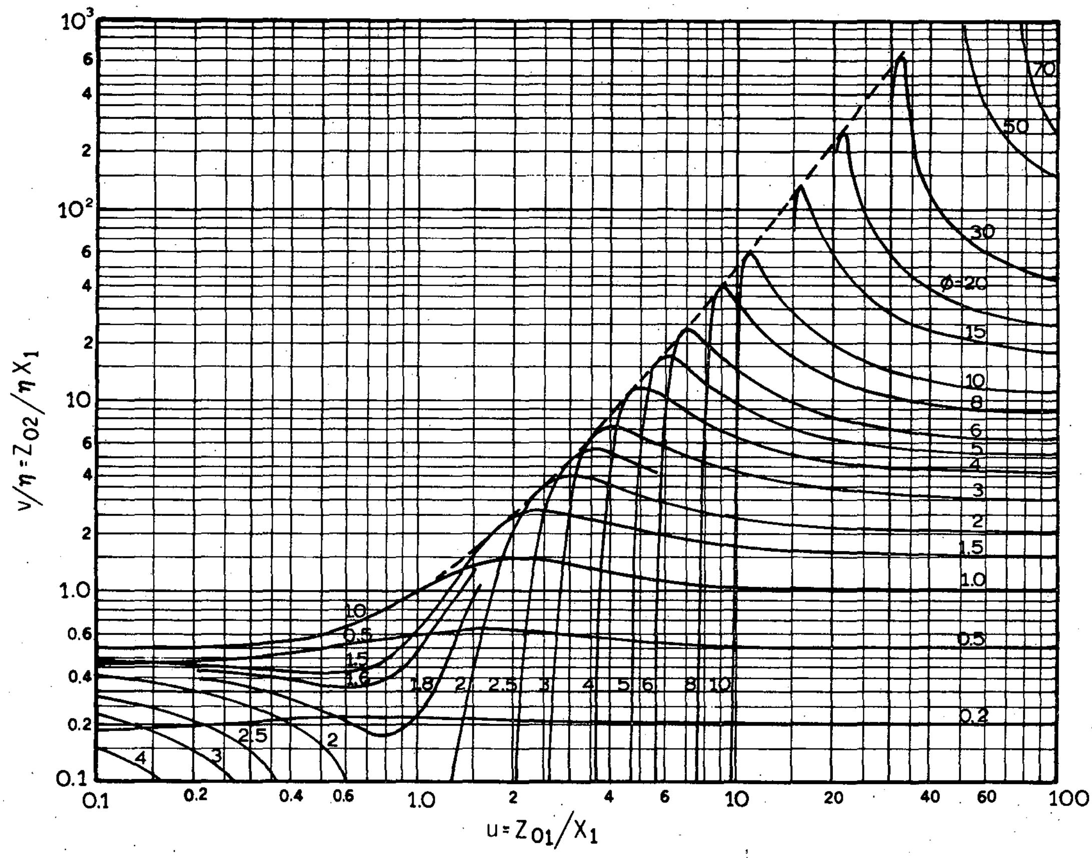

XBL 692 4803

Fig. 4

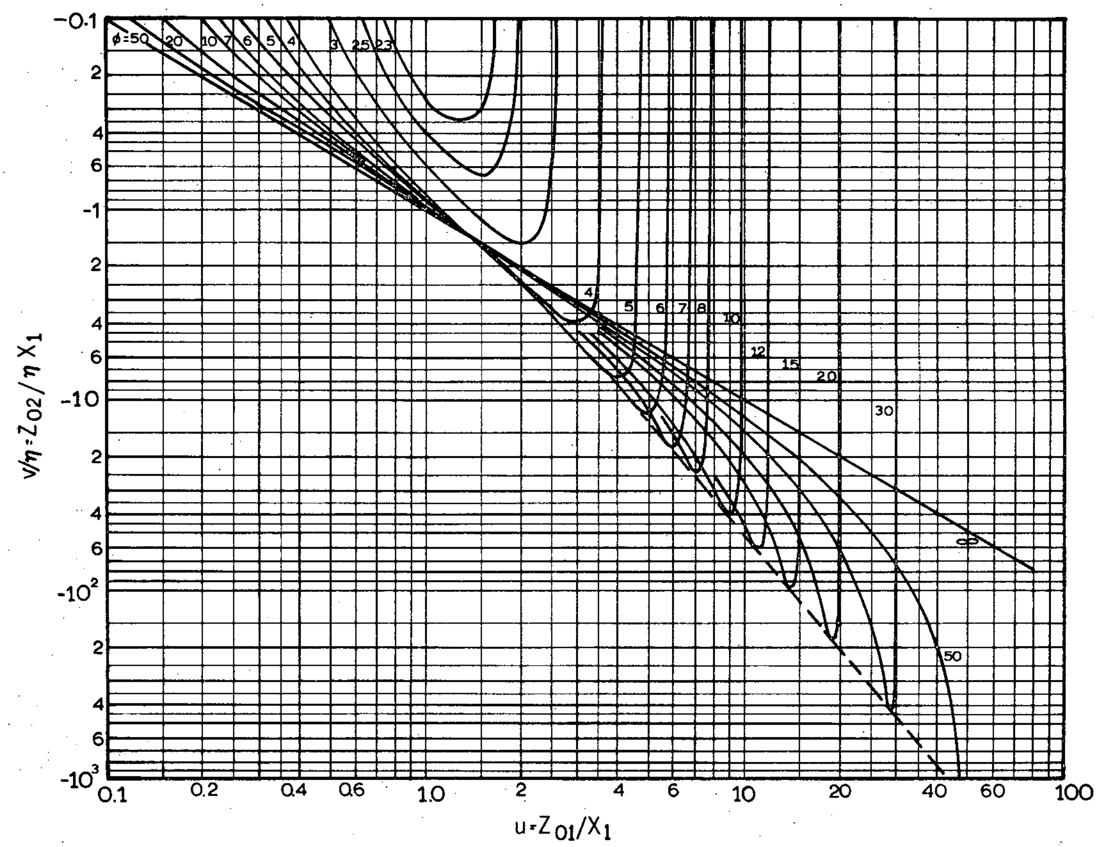

XBL 692 4804

Fig. 5

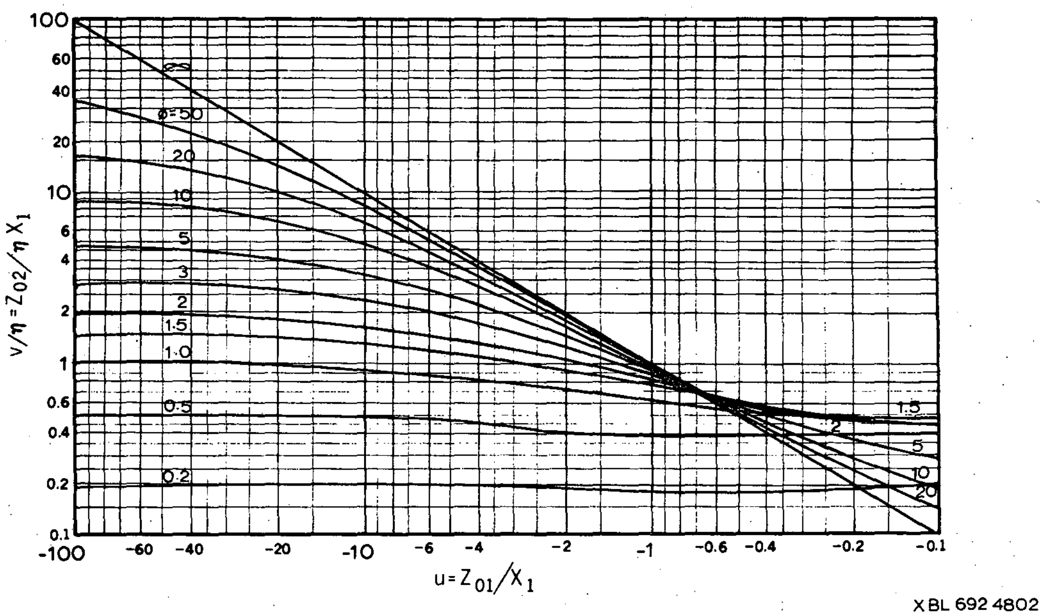
100
60
40
20
10
6
4
2
1
0.6
0.4
0.2
0.1
-100
-60
-40
-20
-10
-6
-4
-2
-1
-0.6
-0.4
-0.2
-0.1
$v/\eta = Z_{02}/\eta X_1$
$u = Z_{01}/X_1$
∞
ø=50
20
10
5
3
2
1.5
1.0
0.5
0.2
1.5
2
5
10
20
XBL 692 4802

Fig. 6

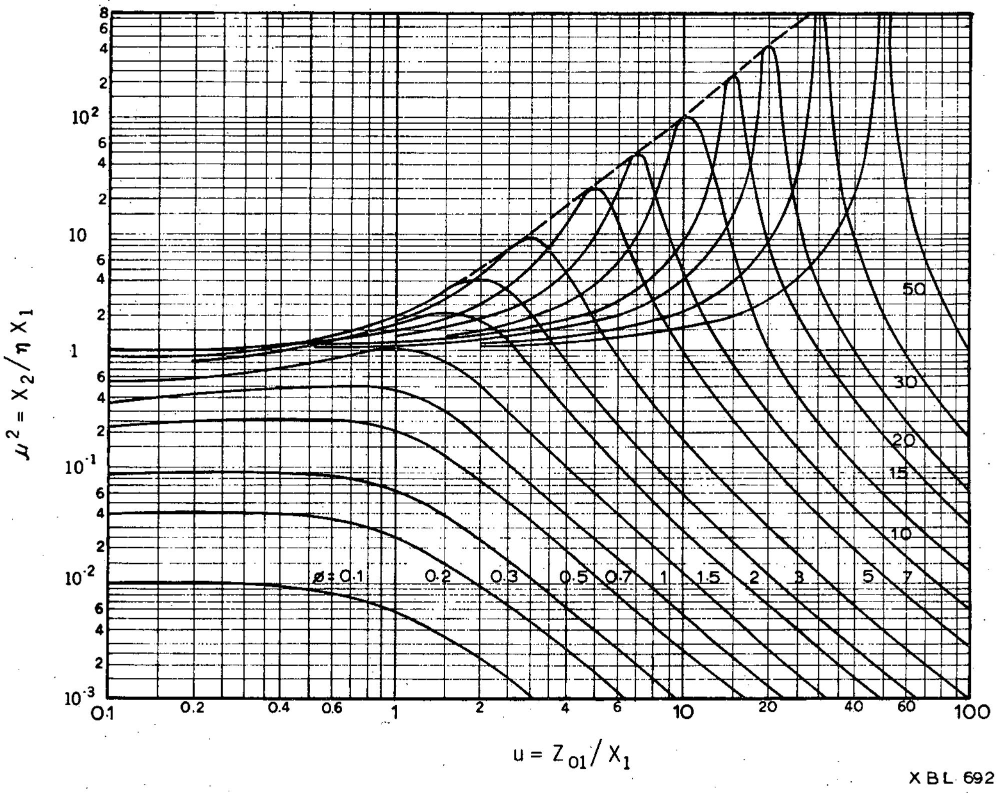
$\mu^2 = X_2/\eta X_1$
$u = Z_{01}/X_1$
ø = 0.1
0.2
0.3
0.5
0.7
1
1.5
2
3
5
7
10
15
20
30
50
XBL 692 4805

Fig. 7

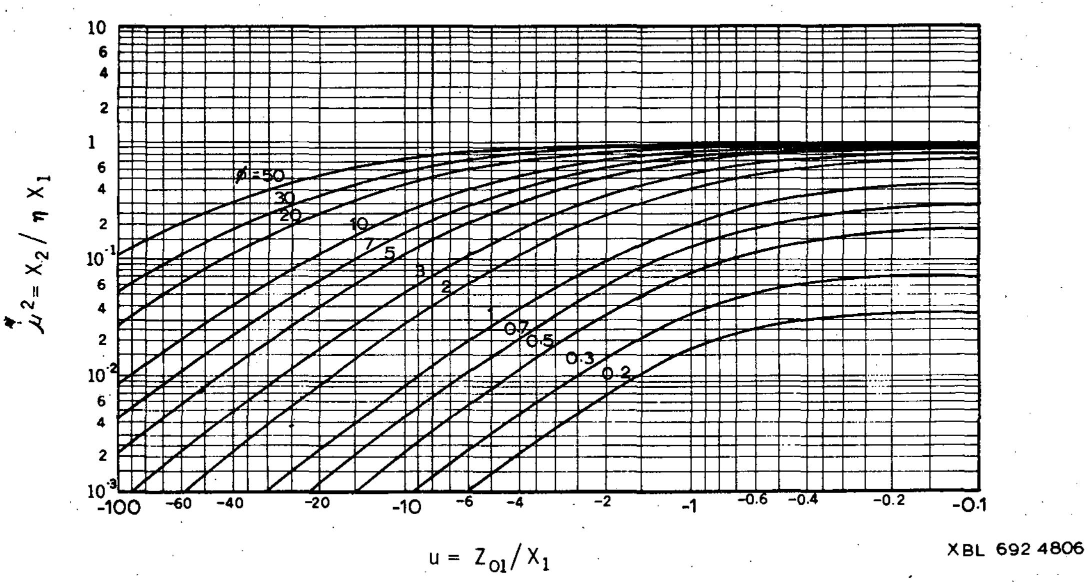
10
6
4
2
1
6
4
2
10^{-1}
6
4
2
10^{-2}
6
4
2
10^{-3}
$\mu^2 = X_2 / \eta X_1$
ϕ=50
30
20
10
7
5
3
2
1
0.7
0.5
0.3
0.2
-100
-60
-40
-20
-10
-6
-4
-2
-1
-0.6
-0.4
-0.2
-0.1
$u = Z_{01}/X_1$
XBL 692 4806

Fig. 8

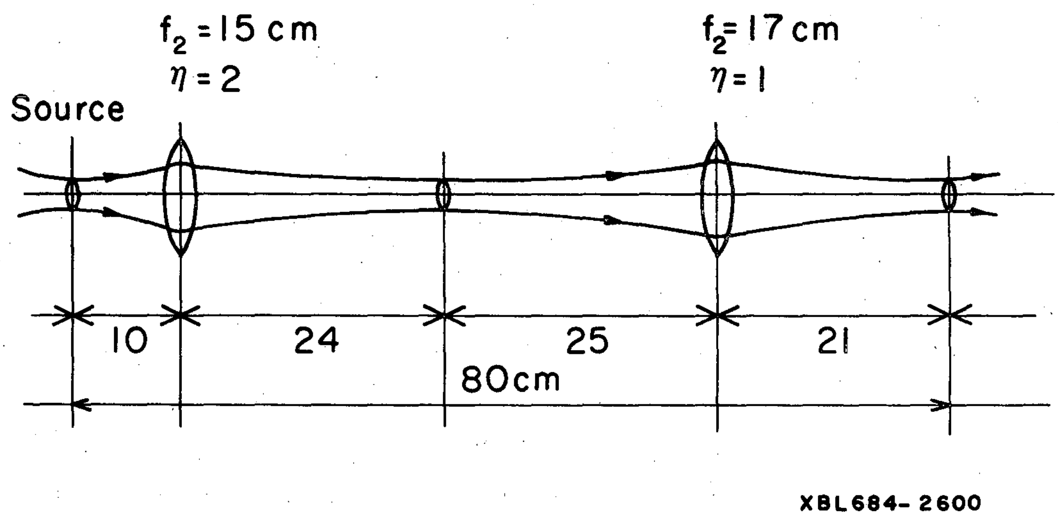

Fig. 9

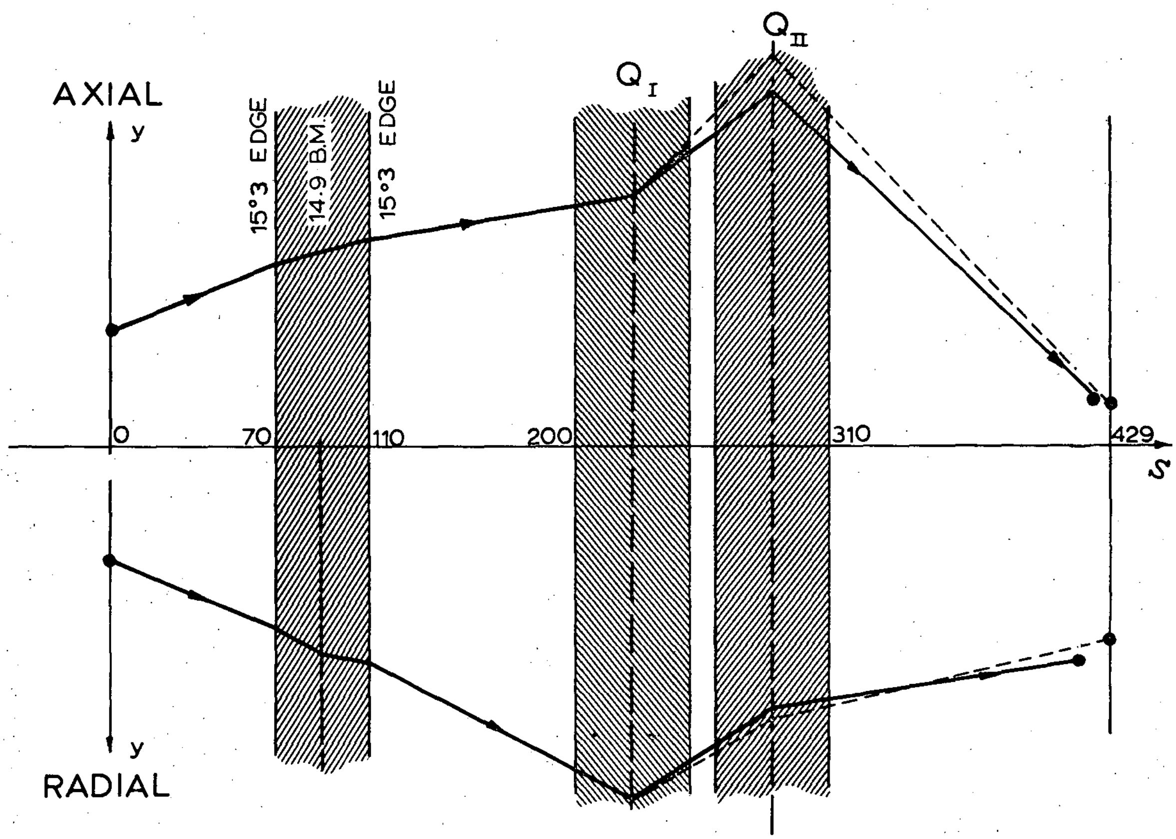

FIG. 10

XBL 699 4886

Fig. 10

TECHNICAL INFORMATION DIVISION
LAWRENCE RADIATION LABORATORY
UNIVERSITY OF CALIFORNIA
BERKELEY, CALIFORNIA 94720